Electronic Supplementary Information for Physical Chemistry Chemical Physics

Supporting Information For

Partially fluorinated MIL-47 and MIL-53 frameworks: influence of functionalization on gas/vapor sorption and breathing properties

Shyam Biswas, Tom Rémy, Sarah Couck, Dmytro Denysenko, Geert Rampelberg, Joeri F. M. Denayer, Dirk Volkmer, Christophe Detavernier and Pascal Van Der Voort*

* To whom correspondence should be addressed. E-mail: pascal.vandervoort@ugent.be; Tel: (+)32-92644442; Fax: (+)32-92644983.

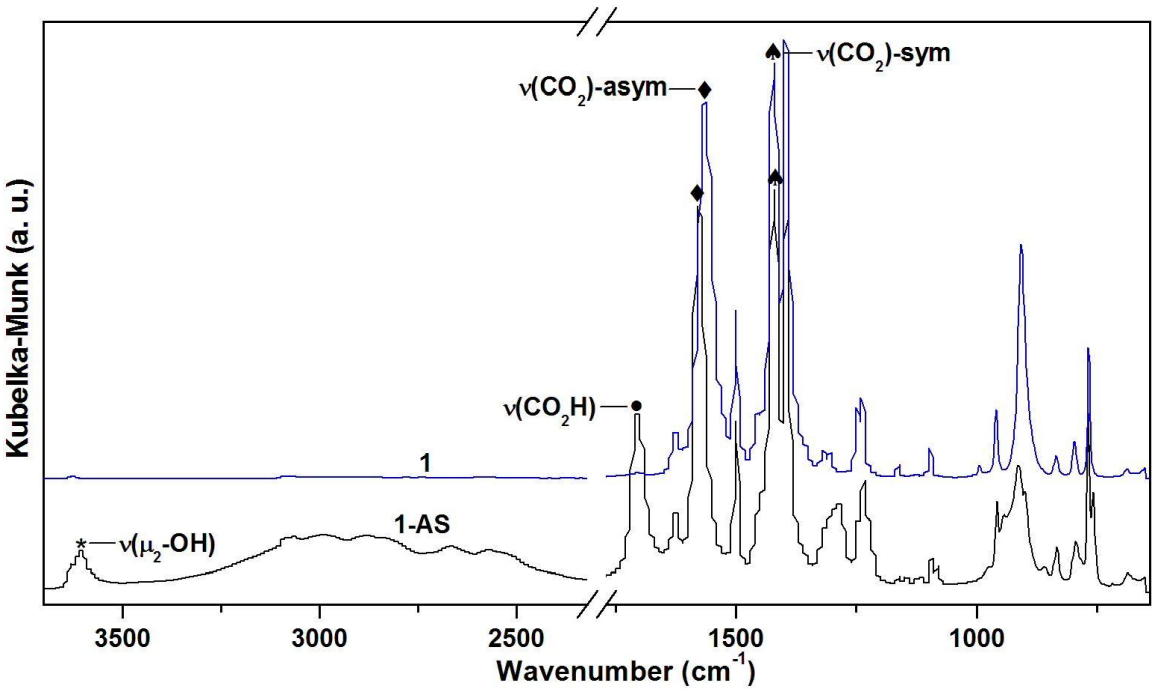

Figure S1. DRIFT spectra of **1-AS** (black) and **1** (blue).

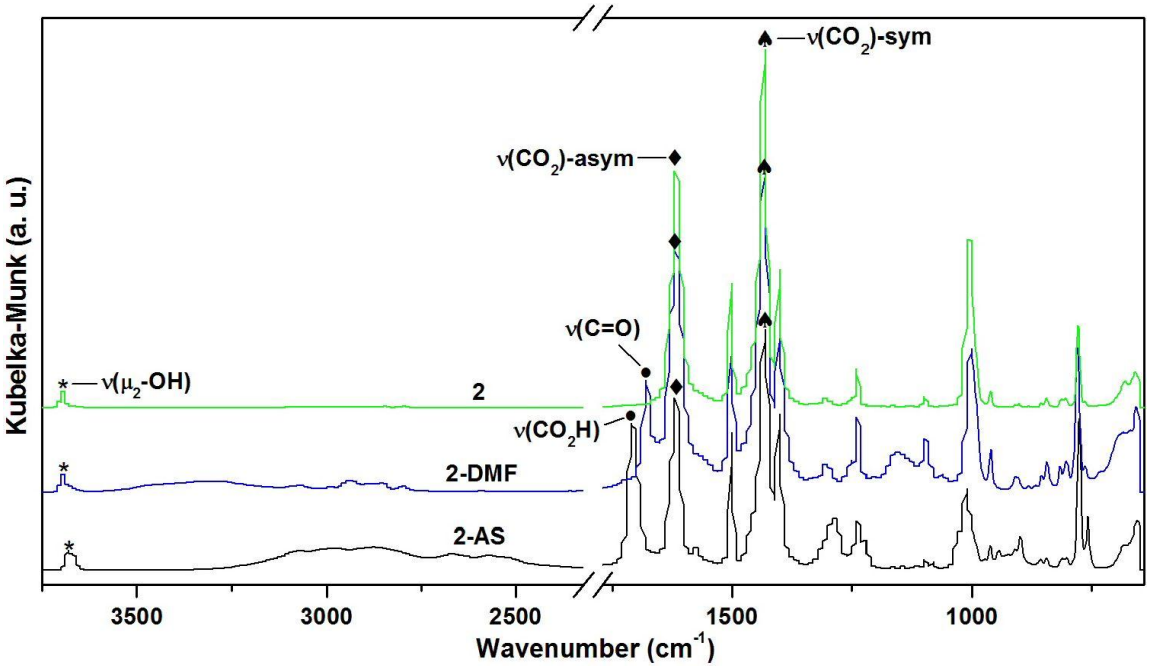

Figure S2. DRIFT spectra of **2-AS** (black), **2-DMF** (blue) and **2** (green).

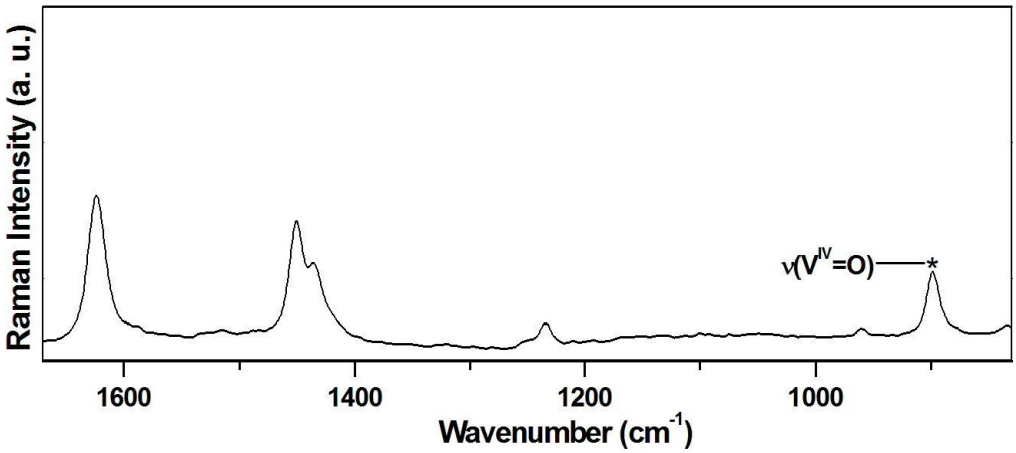

Figure S3. Raman spectrum of thermally activated **1**.

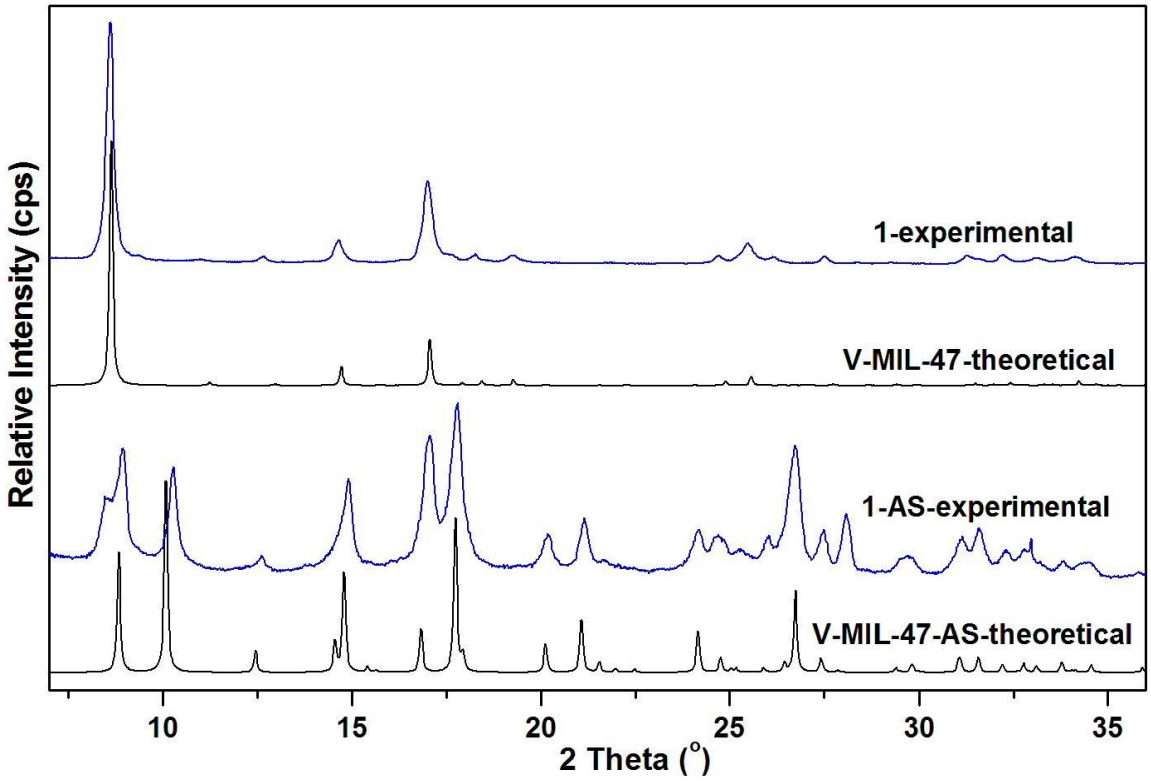

Figure S4. Theoretical (black) and experimental (blue) laboratory XRPD patterns (λ = 1.5406 Å) of the different forms of **1** and V-MIL-47.

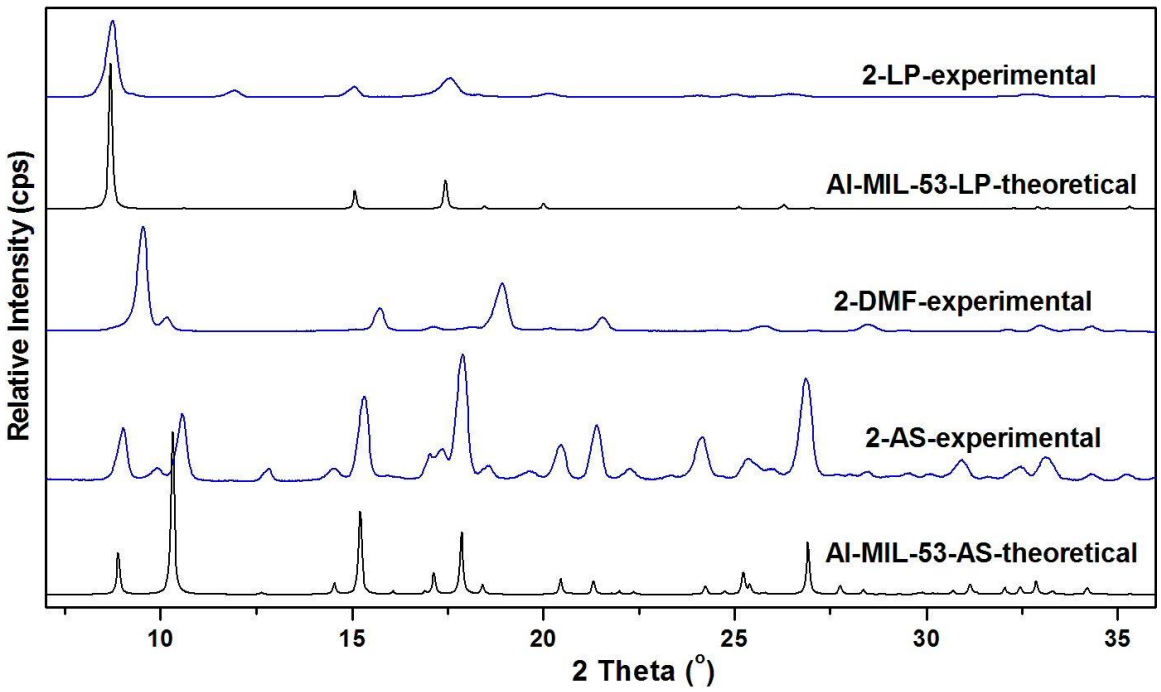

Figure S5. Theoretical (black) and experimental (blue) laboratory XRPD patterns (λ = 1.5406 Å) of the different forms of **2** and Al-MIL-53.

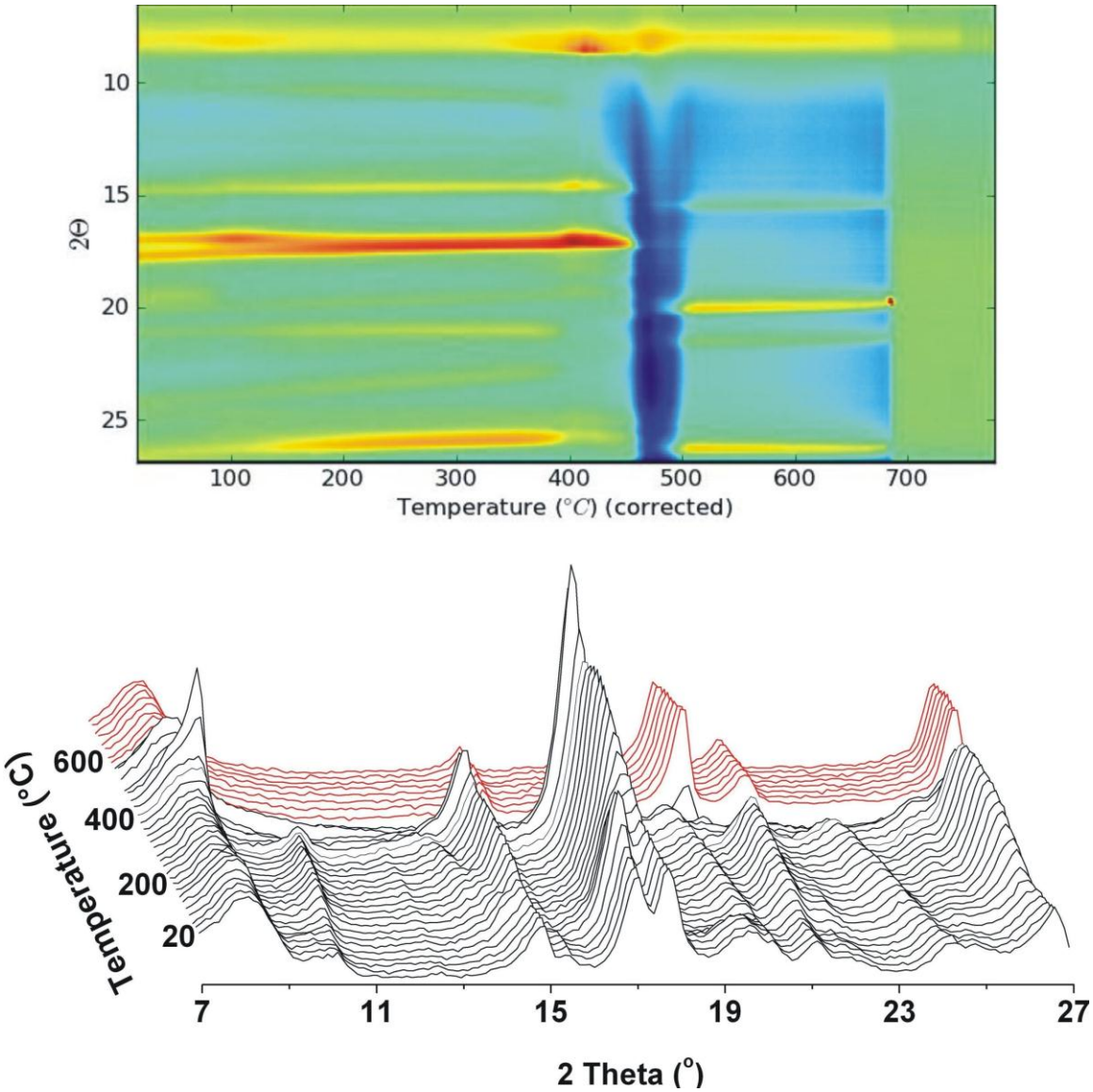

Figure S6. TDXRPD patterns (λ = 1.5406 Å) of **1-AS** measured in air atmosphere in the range of 20–800 ºC. The black and red patterns denote stable and decomposed phases, respectively. The variation of the intensities of the Bragg peaks as a function of temperature is shown on the top.

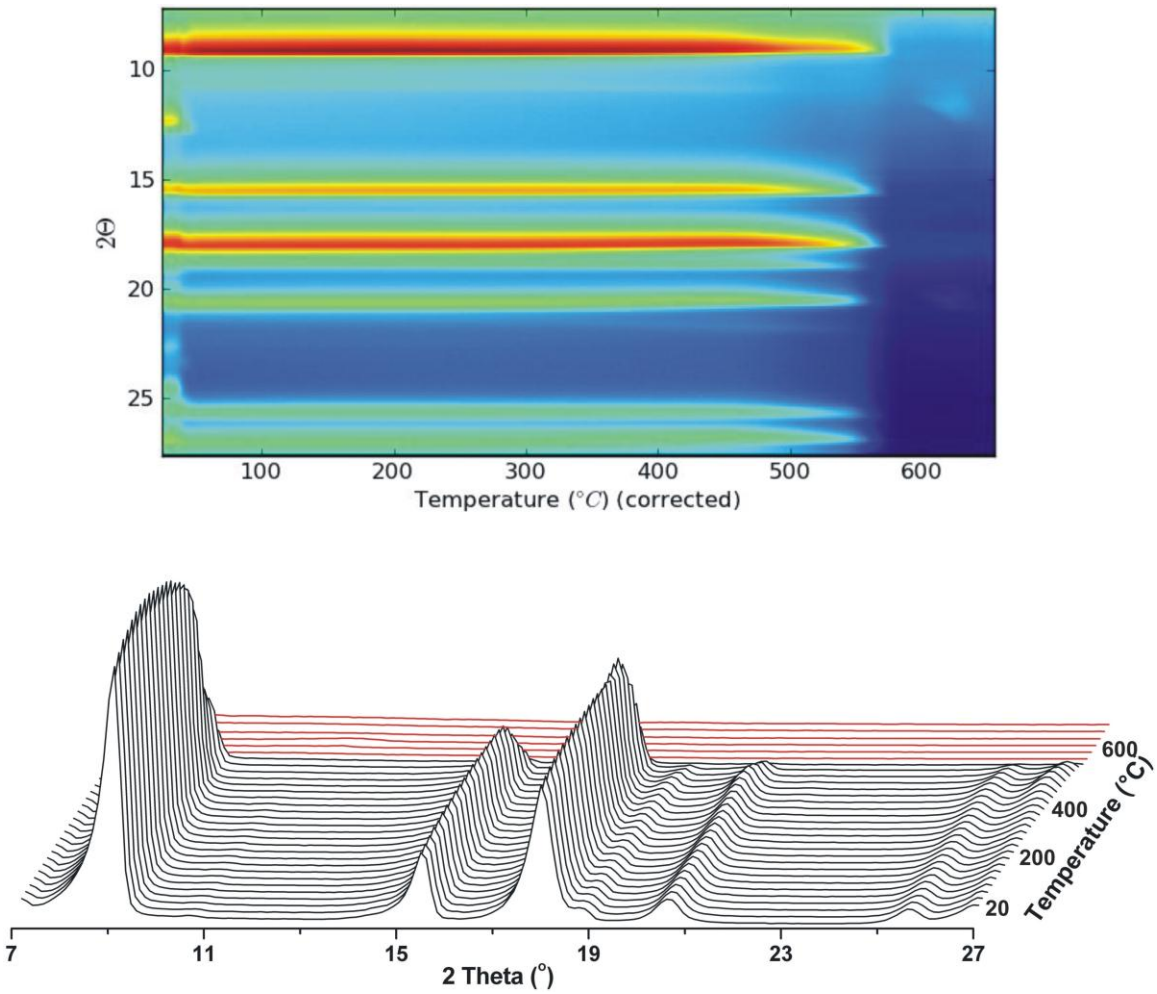

Figure S7. TDXRPD patterns (λ = 1.5406 Å) of the thermally activated form of **2** measured in air atmosphere in the range of 20–650 ºC. The black and red patterns denote stable and decomposed phases, respectively. The variation of the intensities of the Bragg peaks as a function of temperature is shown on the top.

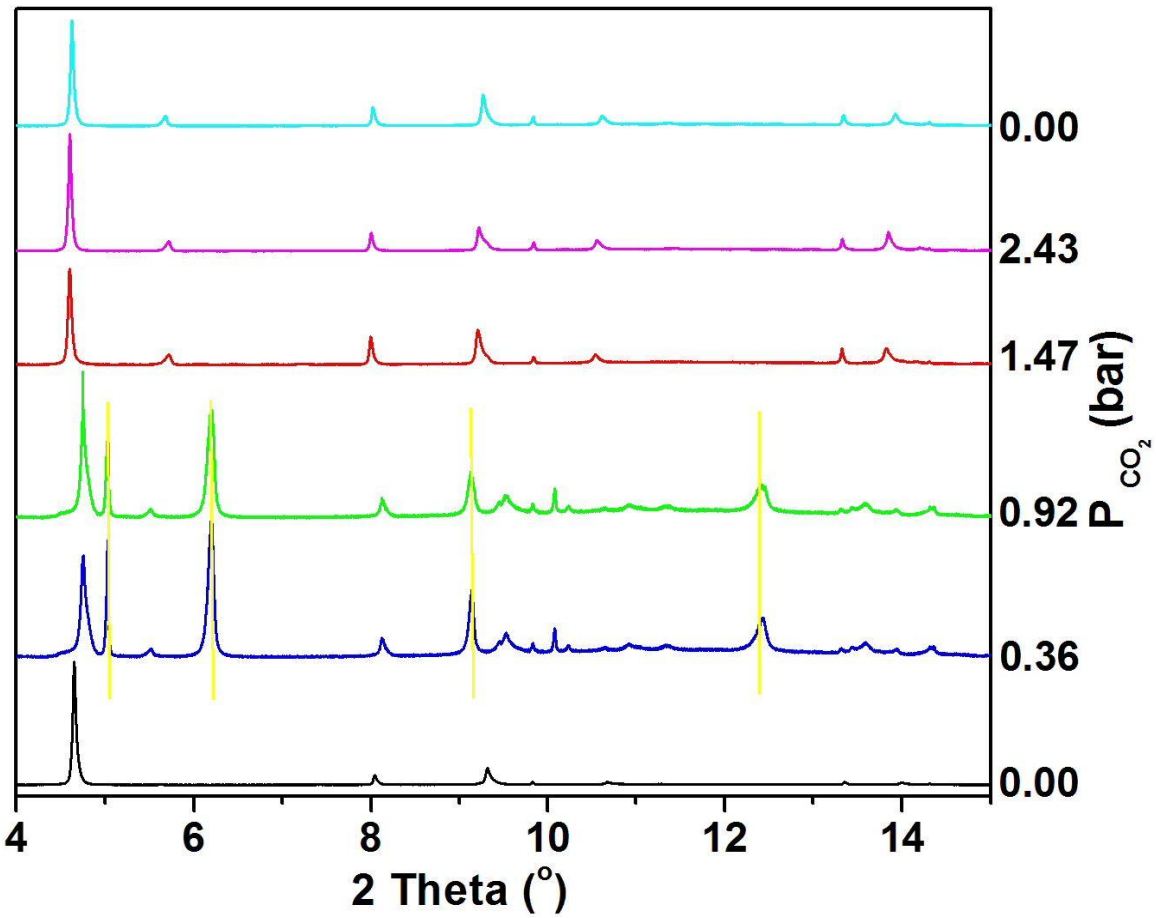

Figure S8. In-situ synchrotron XRPD patterns (λ = 0.827131 Å) of **2** collected at a certain pressure of CO_2 and –40 °C. The Bragg peaks marked by yellow lines indicate the narrow pore phase, whereas the rest of the Bragg peaks denote the large pore phase. Before the measurement, the sample was degassed at 200 °C for 30 min under vacuum.

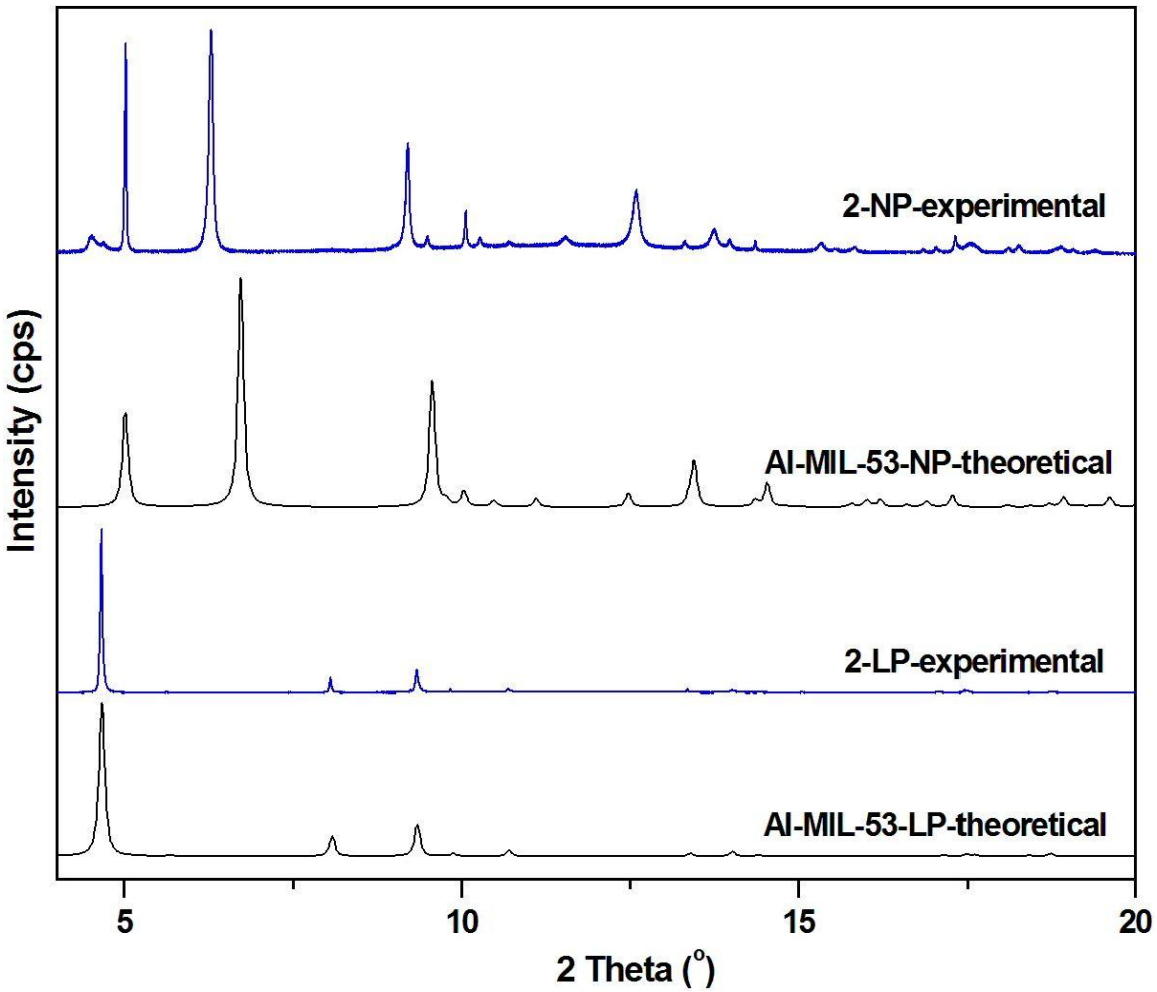

Figure S9. Theoretical (black) and experimental (blue) synchrotron XRPD patterns (λ = 0.827131 Å) of the different forms of **2** and Al-MIL-53. The XRPD patterns for the LP and NP phases of **2** were collected at –80 °C immediately after evacuation and after 5 h of staying under vacuum, respectively.

Table S1. Weight loss steps in TG curves for **1-AS**, **2-AS**, **2-DMF** and their assignments.

Compound	Number of Guest Molecules Removed Below Decomposition Temperature	1st Weight Loss (%): Obs. / Cal.
1-AS	0.3 (H_2BDC-F)	17.0 / 18.1
2-AS	0.5 (H_2BDC-F)	30.3 / 28.9
2-DMF	0.3 DMF	8.8 / 8.8

Table S2. Elemental analyses for **1**, **2** and **2-DMF**.

Compound	Molecular Formula	$C_{obs.}$ / $C_{cal.}$ (%)	$H_{obs.}$ / $H_{cal.}$ (%)
1	$C_8H_3FO_5V$	38.35 / 38.58	1.07 / 1.21
2	$C_8H_4AlFO_5$	42.23 / 42.49	1.64 / 1.78
2-DMF	$C_{8.9}H_{6.1}AlFN_{0.3}O_{5.3}$	43.36 / 43.09	2.29 / 2.47

Table S3. Frequencies of DRIFT bands[a] for **1**, **2** and **2-DMF**.

Compound	Frequencies (cm^{-1}) of DRIFT Bands
1	3628 (w), 1623 (w), 1564 (vs), 1500 (s), 1426 (vs), 1397 (sh), 1318 (w), 1298 (sh), 1249 (sh), 1238 (m), 1160 (w), 1101 (w), 997 (w), 958 (m), 908 (vs), 834 (w), 794 (m), 770 (s), 686 (w), 651 (w)
2	3699 (m), 1619 (vs), 1498 (s), 1428 (vs), 1401 (s), 1303 (w), 1240 (m), 1101 (w), 1004 (vs), 959 (w), 843 (w), 805 (w), 777 (s), 680 (sh), 659 (m)
2-DMF	3693 (m), 3307 (br), 2935 (w), 1681 (s), 1618 (vs), 1498 (s), 1428 (vs), 1398 (s), 1309 (w), 1240 (m), 1158 (m), 1102 (m), 995 (s), 956 (m), 905 (w), 849 (w), 804 (w), 779 (s), 654 (m)

[a] Abbreviations: s = strong; vs = very strong; m = medium, w = week, sh = shoulder.

Table S4. Selected frequencies (cm^{-1}) of DRIFT bands for the different forms of **1** and **2**.

Compound	Asymmetric Stretching of $–CO_2$ Group	Symmetric Stretching of $–CO_2$ Group	Stretching of $–CO_2H$ Group	Stretching of –OH Group
1-AS	1579	1418	1706	3603
1	1565	1418	-	-
2-AS	1619	1429	1709	3681
2	1619	1429	-	3694
2-DMF	1619	1432	-	3699